ÓBUDAI EGYETEM
ÓBUDA UNIVERSITY

Doctoral School on Materials Sciences and Technologies

The Effect of Ultrasound on the Inelastic Deformation of Metals

by

Ali H. Alhilfi

M.Sc. in Materials Sciences and Engineering

Supervisor

Prof. Dr. habil. Endre Ruszinkó

University professor, Óbuda University

Budapest 2023

I. Introduction

Since the early 20th century – Austrian scientists Blaha and Langenecker conducted the first tensile tests with superimposed ultrasound on a Zinc single crystal – the ultrasound-assisted processes have received rapidly increasing interest from academics and industries. Ultrasonic technology is a convenient and accessible assisting tool for many metalworking processes, such as machining, forming, joining, welding, microelectronic wire bonding, etc. Ultrasound shows various benefits: low energy consumption, high reliability and ampacity, short process time, etc. In addition, ultrasound finds ever-growing applications in the phase transformation processes of shape memory alloys.

II. Objectives

A. The effect of ultrasound on plastic deformation

Acoustic Temporary Softening.

Acoustic Residual Effects – residual hardening or softening.

B. The effect of ultrasound on the temporary processes

Ultrasound-assisted creep.

Ultrasound-assisted relaxation of the cold-worked materials.

C. The effect of ultrasound on the phase transformation in shape memory alloys

Ultrasound-assisted austenite transformation (*transformation plasticity*).

Martensite transformation (pseudo elasticity) coupled with ultrasound energy.

Despite numerous experimental and numerical analyses about the potential benefits of applying ultrasonic energy, the underlying physical principles remain elusive. Two categories of the interpretation of the ultrasound effects can be indicated: (i) ***stress superposition*** and (ii) ***direct acoustic softening***.

The phenomena considered above have been modeled in terms of the Synthetic theory of inelastic deformation, whose short review is presented below.

III. The Synthetic Theory of Inelastic Deformation

Inelastic deformation at a point of the body is determined via deformations at the micro level of material, i.e., as a sum of inelastic deformations developed in active microvolumes:

$$\vec{\boldsymbol{e}} = \iiint_V \varphi_N \vec{\boldsymbol{N}} dV\,, \tag{3.1}$$

$$d\psi_N = r d\varphi_N - K\psi_N dt, \tag{3.2}$$

$$\psi_N = \left(\vec{\boldsymbol{S}} \cdot \vec{\boldsymbol{N}}\right)^2 - I_N^2 - S_P^2, \tag{3.3}$$

$$I_N(t) = B\int_0^t \frac{d\vec{\boldsymbol{S}}}{ds}\cdot\vec{\boldsymbol{N}}\exp\big(-p(t-s)\big)ds\,, \tag{3.4}$$

where B and p are model constants.

While Eqs. (3.2)-(3.4) are applied for the modeling of plastic/creep deformation, for the case of phase transformations, the strain intensity is defined via the rate of martensite fraction (Φ) as

$$r\dot{\varphi}_N = \dot{\Phi}. \tag{3.5}$$

For martensite transformation, $\dot{\Phi}$ is

$$\dot{\Phi} = -\frac{\dot{T}_e}{M_s - M_f}, \qquad \dot{T}_e < 0 \text{ and } M_f < T_e < M_s. \tag{3.6}$$

For austenite transformation, $\dot{\Phi}$ is

$$\dot{\Phi} = -\frac{\dot{T}_e}{A_f - A_s}, \qquad \dot{T}_e > 0 \text{ and } A_s < T_e < A_f, \tag{3.7}$$

T_e is effective temperature defined as

$$T_e = T\big(1 - D\vec{\boldsymbol{S}}\cdot\vec{\boldsymbol{N}}\big), \tag{3.8}$$

IV. Results I

In terms of the Synthetic theory, a model for the analytical description of the plastic flow of metals in the ultrasound field has been developed. The proposed extension of the Synthetic theory leads to correct results when considering the following phenomena:

(i) Stress drop on the stress~strain diagram as the ultrasound is On

(ii) Acoustoplasticity – stress~strain diagrams under the simultaneous action of unidirectional and vibrating load

(iii) Ultrasound residual hardening/softening – stress~strain diagram for the post-sonicated state of the metals

Eq. (3.3) is extended by two terms, U_t and U_r:

$$\psi_{NU} = H_N^2 + U_t^2 + f(\gamma)U_r^2 - S_S^2, \tag{4.1.1}$$

U_t is presented as a product of ultrasound energy (power function) and sonication duration (exponential function):

$$U_t = A_1 U^{A_2}(2 - e^{-wt})\left(\vec{\boldsymbol{u}} \cdot \vec{\boldsymbol{N}}\right), \qquad t \in [0, \tau] \tag{4.1.2}$$

U_r is defined as

$$U_r = h(\varepsilon - U) \times A_3 \int_0^{\tau} U^{A_4} dt\,, \tag{4.1.3}$$

Formula (3.2), which reduces to $\psi_N = r\varphi_N$ in the case of plastic deformation, together with (4.1.1) and (4.1.2), gives the strain intensity in the presence of ultrasound (φ_{NU}) as

$$\varphi_{NU} = \left(\vec{\boldsymbol{S}} \cdot \vec{\boldsymbol{N}}\right)^2 + A_1 U^{A_2}(2 - e^{-wt})\left(\vec{\boldsymbol{u}} \cdot \vec{\boldsymbol{N}}\right) - S_S^2, \tag{4.1.4}$$

After the ultrasound is Off, due to the formula (4.1.3), the plastic strain intensity takes grows in the following form

$$\Delta\varphi_N = \left(\vec{\boldsymbol{S}} \cdot \vec{\boldsymbol{N}}\right)^2 + f(\gamma)\frac{3}{2}[A_3 U^{A_4}\tau]^2 - S_S^2 - \varphi_{NU}. \tag{4.1.5}$$

The model results obtained correctly correlate with the following experimental recordings:

(i) The magnitude of the stress drop caused by the switching of the ultrasound increases with the ultrasound intensity: Fig. 4.1.

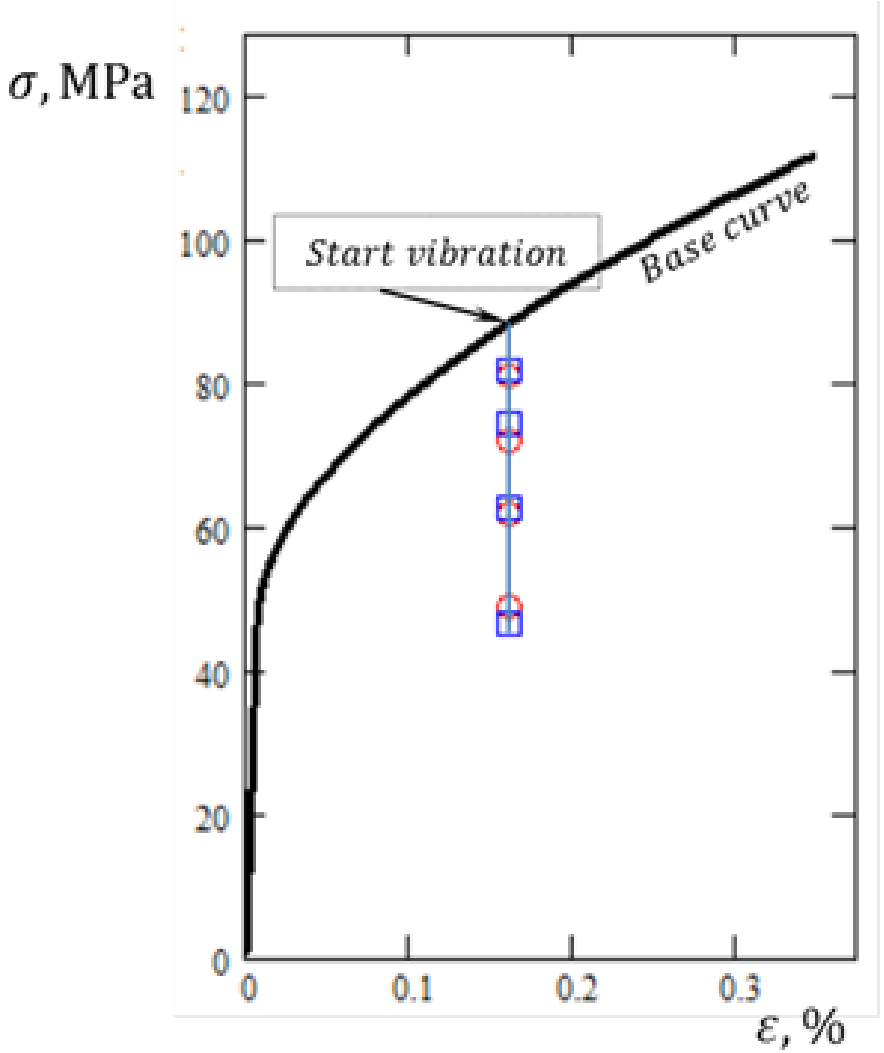

Fig.4.1 Stress drops on the stress-strain diagram of aluminum caused by the switching of ultrasound with different intensities: *Uk*=5.89, 22.0, 60.33, 126.6Jm3

(ii) The material flow with superimposed ultrasound occurs at fewer stress values than the static load alone: Fig. 4.2, portions 2-3 and 6-7. The decrease in static stress increases with the ultrasound intensity/ amplitude: see Figs. 4.4 and 4.5.

(iii) The extended synthetic theory catches the phenomenon of residual hardening: see 3-4 portion in Fig. 4.2, where the plastic deformation in the post-sonicated state develops at greater stress values compared to the case of static loading. At the same time, too short sonification ($\tau = 2$ s for 6-7-8 portion) gives no residual hardening effect, which is explained by the ultrasound energy is not enough to nucleate such a stable defect structure to hamper the plastic flow in the post-sonicated state.

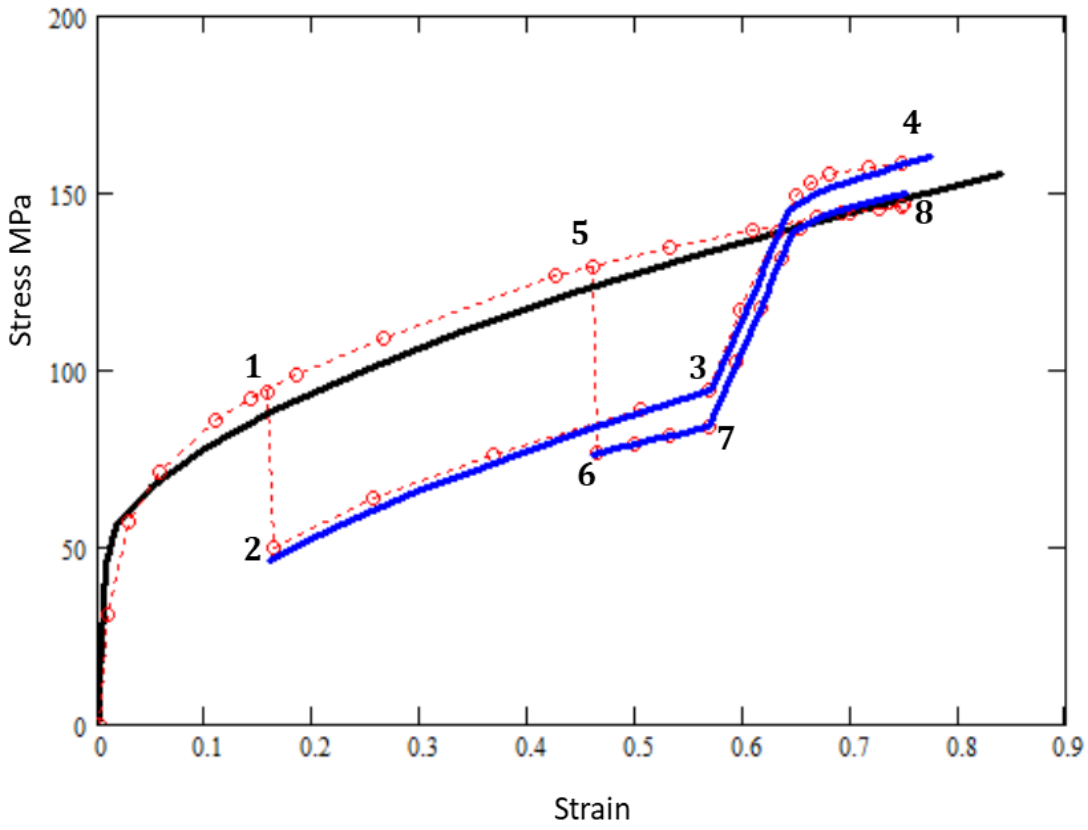

Fig.4.2 Vibration-assisted stress~strain diagrams for aluminum in compression for ultrasound intensity U=126.6Jm3; sonication time τ=8 s for 2-3-4 portion and τ=2 s for 6-7-8 portion; lines – model, ○ – experiment (Yao et al., 2012)

(iv) The model results for residual hardening are presented in Fig. 4.3, where the stress~strain diagram after the sonication runs beneath that obtained for the static load alone.

(v) Figs. 4.4 and 4.5 show the residual hardening for aluminum (high SFE) and residual softening for titanium (low SFE). With the increase in ultrasound amplitude, both phenomena appear more clearly.

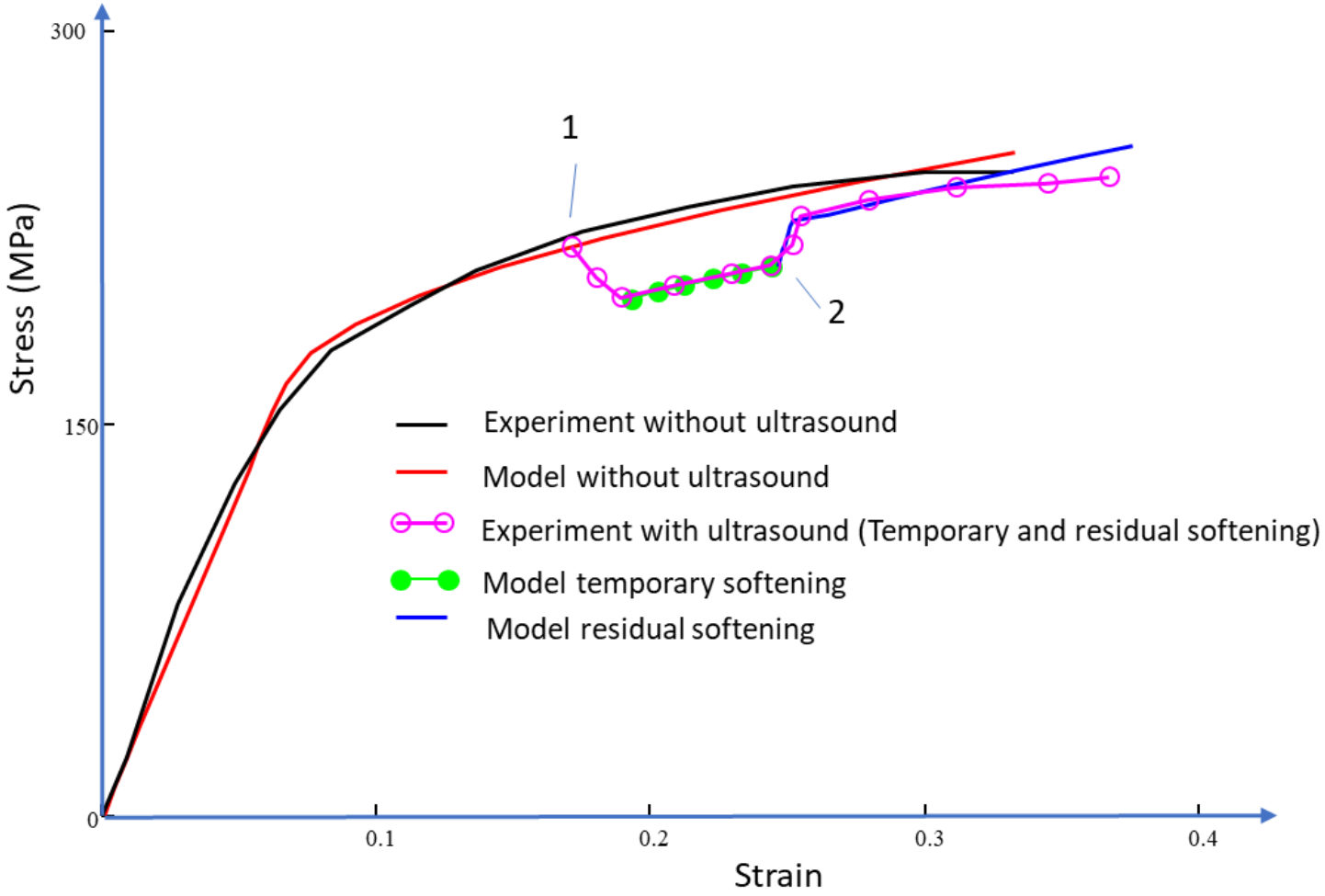

Fig. 4.3 Vibration-assisted stress~strain compression diagrams for copper; ultrasound amplitude 1.3 μm.

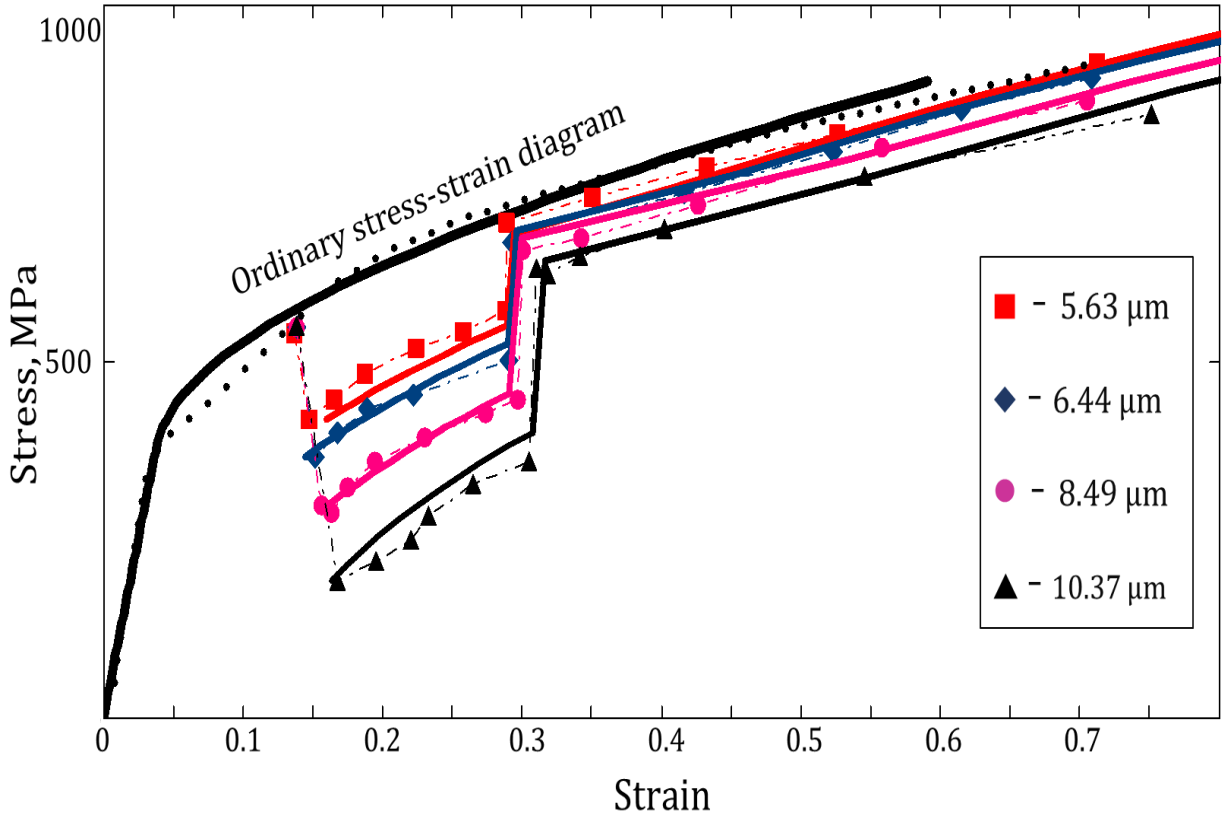

Fig. 4.5 Stress~strain compression diagrams for titanium in the ultrasonic field (points – experimental data, Zhou et al. (2017); lines – model curves).

Fig. 4.4. Stress~strain compression diagrams of aluminum in the ultrasonic field (points – experimental data, Zhou et al. (2017); lines – model curves).

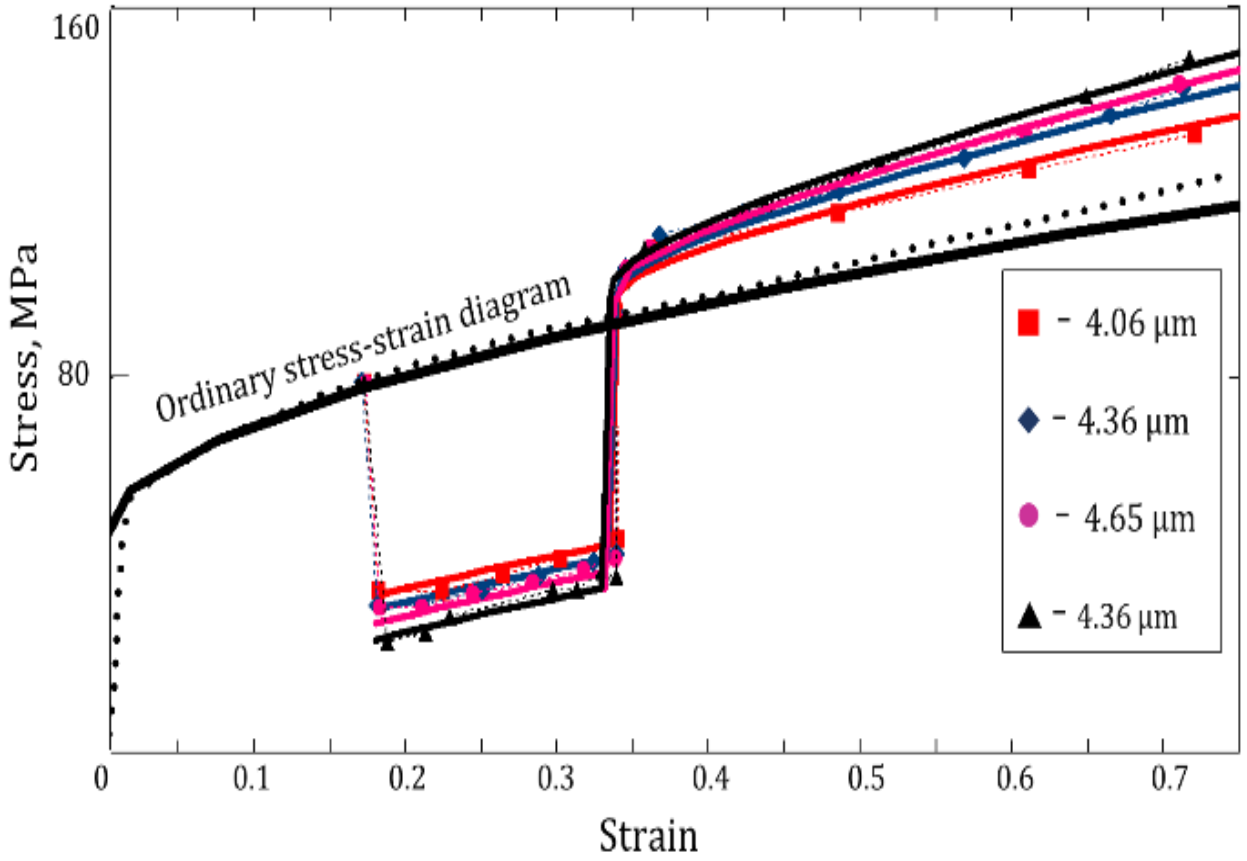

V. Results II

In terms of the Synthetic theory, a model for the analytical description of the ultrasound-assisted temporary deformation processes has been developed. The obtained results show good conformity between the model and experimental data for the following phenomena:

(i) The increase in primary creep under the periodic and continuous action of ultrasound

(ii)The increase in secondary creep in an acoustic field

(iii)Ultrasound-induced relaxation (recovery) of the work-hardened materials

Adhering to the overall concept of modeling ultrasound's effect on inelastic deformation, the basic relationship of the synthetic theory, Eq. (3.3), is to be extended by the term (U_C) responsible for acoustic energy:

$$\psi_N = H_N^2 - I_N^2 - S_P^2 + U_C^2, \tag{4.2.1}$$

$$U_C = \vec{\boldsymbol{u}} \cdot \vec{\boldsymbol{N}}, \tag{4.2.2}$$

$$\vec{\boldsymbol{u}} = A_1 {S_m}^{A_2} (1 - e^{-wt}) \vec{\boldsymbol{u}}, \tag{4.2.3}$$

To catch the phenomena recorded at the superposition of ultrasound on the A) secondary creep and B) the relaxation processes, the following is proposed.

A) The creep rate within one slip system is obtained from (3.2) as $r\dot{\varphi}_N = K\psi_N$.

B) The relaxation of work-hardened material, i.e., the decrease in the defects cumulated in plastic flow, is derived from (3.2) as $d\psi_N = -K\psi_N dt$.

In order to reflect an accelerating effect of the acoustic energy on the above processes, the function K from (3.2) is extended by the term containing the ultrasound stress amplitude S_m:

$$K_U = K + A_1 (S_m H_{\max})^{A_2}, \tag{4.2.4}$$

The model results obtained derived from (3.1) and (4.2.1)-(4.2.4) – show good agreement with the following experimental data:

(i) Ultrasound energy increases the primary creep deformation: see Figs. 4.6 and 4.7. Fig. 4.6 demonstrates that this phenomenon escalates with the ultrasound stress amplitude.

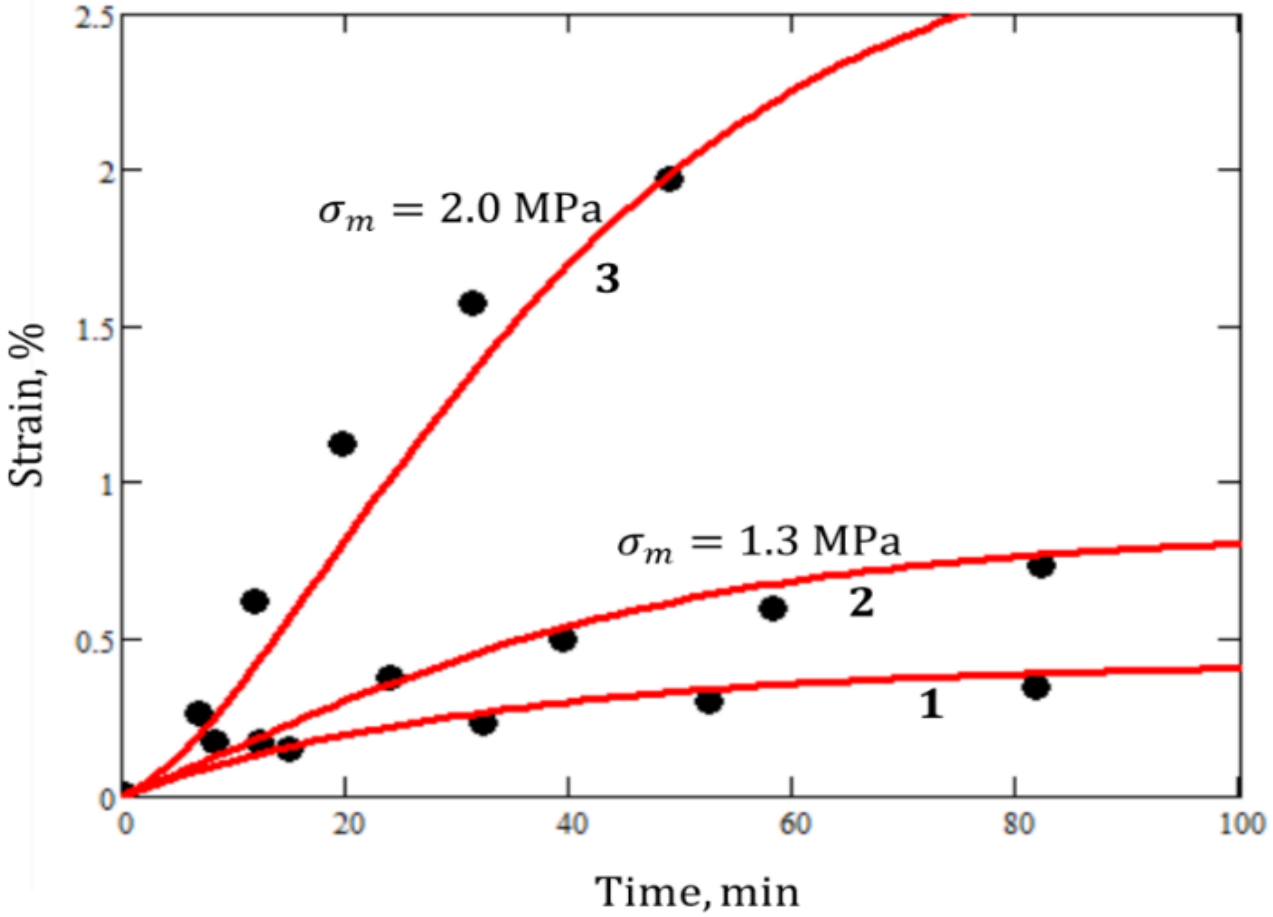

Fig. 4.6 Strain vs. Time diagrams of aluminum in uniaxial tension ($\sigma = 10$ MPa, $T = 40$°C): 1 – ordinary creep, 2 and 3 – ultrasound-assisted creep with continuous sonication, • – experiment (Kulemin, 1978), lines – model.

(ii) In the case of periodic sonication (Fig. 4.7), the values of deformation increments decay with the number of ultrasound switches, and there comes the point when the ultrasound exerts no effect. In this phenomenon, the temporary behavior of ultrasound defects (their number first increases and then goes to saturation) is most evident.

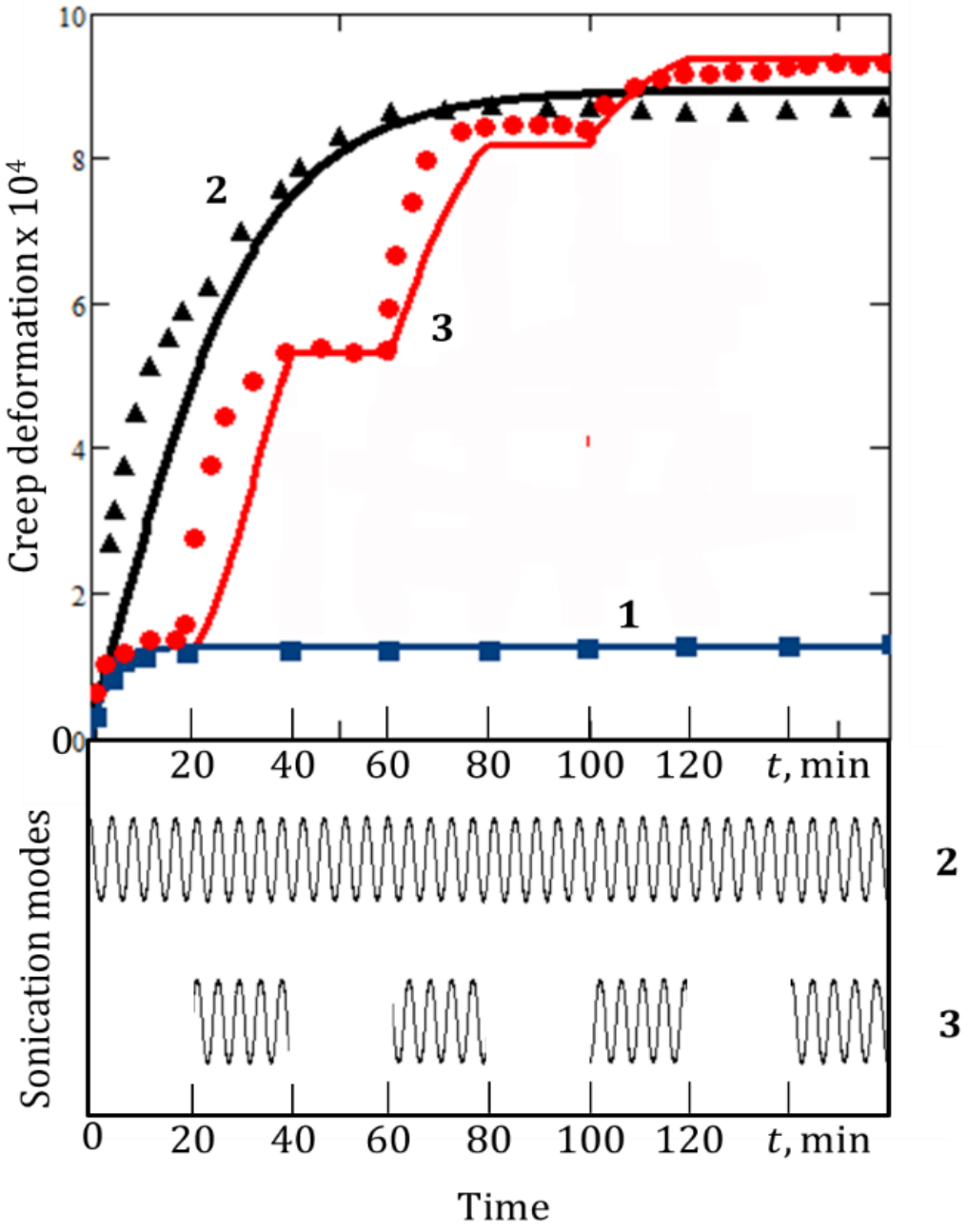

Fig. 4.7 Strain vs. Time diagrams of copper: **1** – ordinary creep, **2** – ultrasound-assisted creep ($\sigma_m = 2.6$ MPa) with continuous sonication, **3** – ultrasound-assisted creep with periodic sonication; symbols – experiment (Kulemin, 1978), lines – model.

(iii) Ultrasound superimposition causes an increase in primary and secondary creep deformation, which is seen in the increase of the slope angle of creep diagrams in Fig. 4.8.

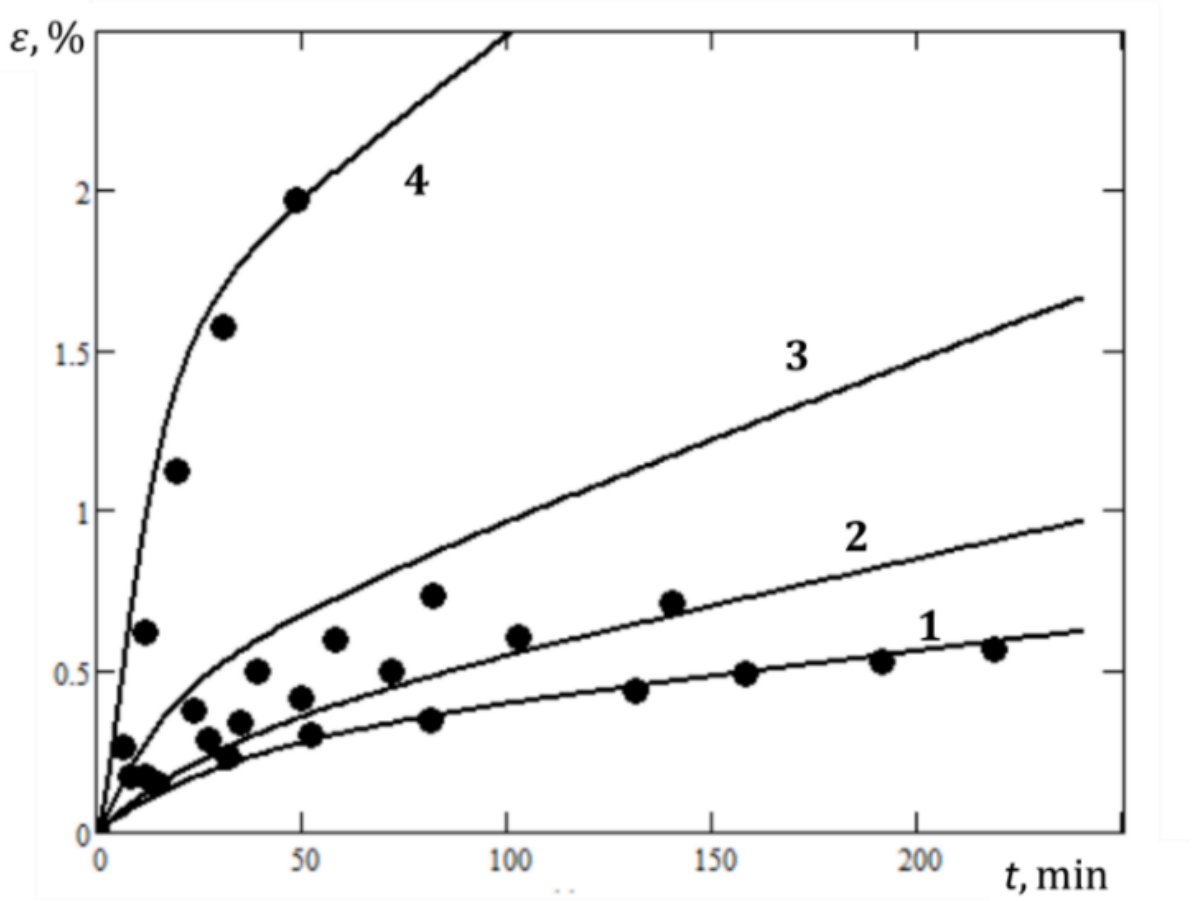

Fig. 4.8 Creep diagrams of aluminum in uniaxial tension ($\sigma = 10$ MPa, $T = 40$°C), 1 – ordinary creep, 2-4 ultrasound-assisted creep with oscillating stress amplitudes of 0.6 MPa (2), 1.3 MPa (3), and 2.0 MPa (4); ● – experiment (Kulemin, 1978), lines – model.

(iv) Ultrasound energy induces the relaxation processes for the materials subjected to plastic deformation, which becomes more evident as plastic deformation grows. So, Line 2 in Fig. 4.9 shows a steeper hardness decrease than Line 1 (without the ultrasound, the recovery of the work-hardened material at room temperature is not observed).

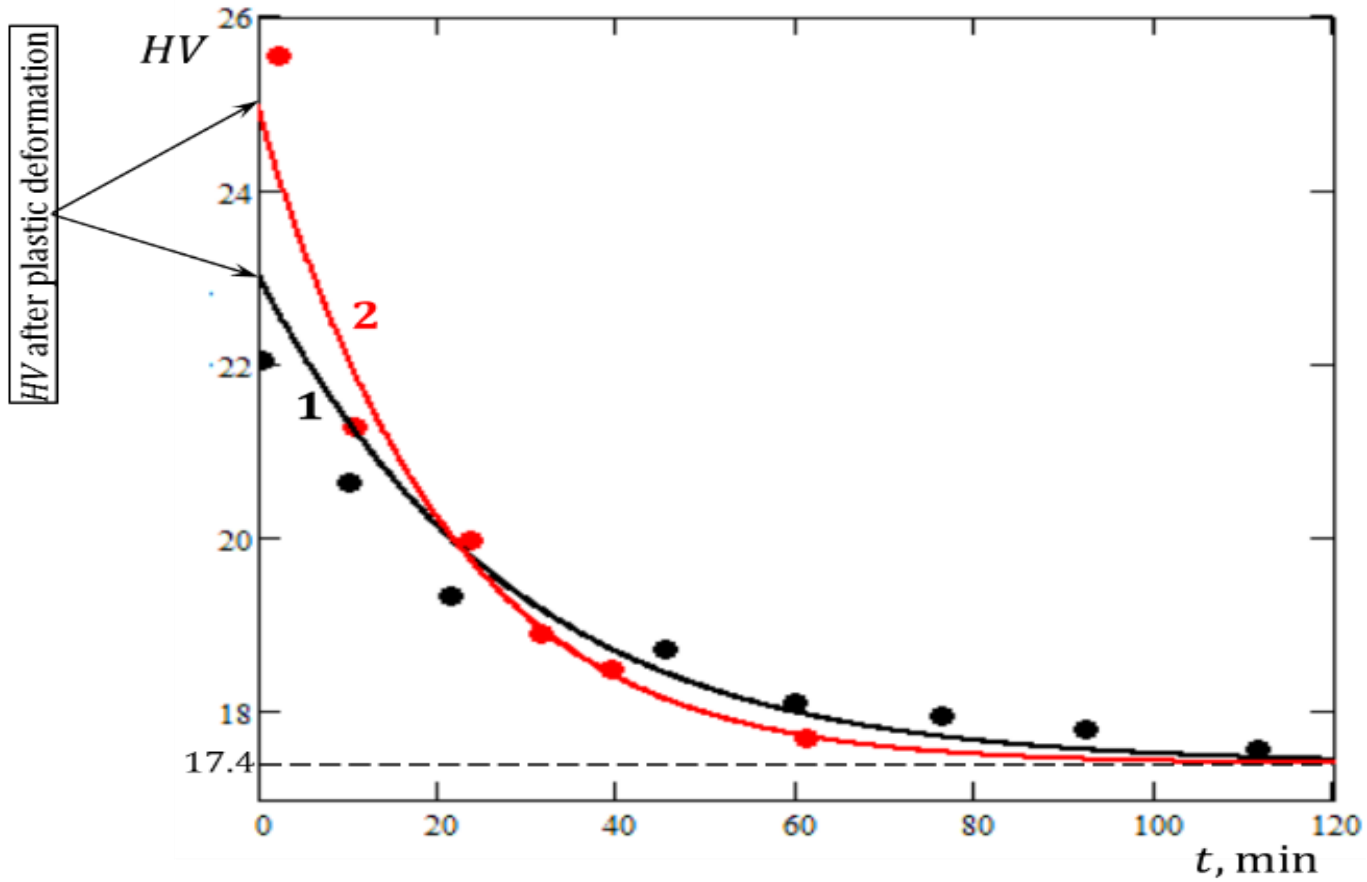

Fig. 4.9 *HV* vs. *sonication time* plots for the plastically deformed aluminum specimen: $\varepsilon_1 = 3.6$ % and $\varepsilon_2 = 6.8$ %, $t = 20$°C; • – experiment (Kulemim, 1978), lines – model

VI. Results III

In terms of the Synthetic theory, a model for the analytical description of the ultrasound-assisted phase transformations of the shape memory alloys has been developed. The model results correctly correlate with experimental recordings for the following phenomena:

(i) Ultrasound impulses induce strain drops during austenite transformation (transformation plasticity)

(ii) Ultrasound superimposed on a static load decreases stresses needed to start martensite transformation during pseudoelastic deformation

To extend the relationship for T_e by a term reflecting the presence of ultrasound:

$$T_e = T\left(1 - D\vec{\boldsymbol{S}} \cdot \vec{\boldsymbol{N}}\right) \pm U, \tag{4.3.1}$$

where the sign "+" is applied for austenite and "–" for martensite transformation.

For ultrasound-assisted transformation plasticity, $\sigma = const$ and $\dot{T} > 0$, the following formulae are proposed

$$U = \left(B + e^{-w(T-T_i)}\right) \int_{A_s}^{T} (f \cdot g) dt\,, \tag{4.3.2}$$

$$f = U_1\left(\vec{\boldsymbol{S}}_m \cdot \vec{\boldsymbol{N}}\right), \tag{4.3.3}$$

$$g = \frac{a^3}{a^2 + (T - C)^2}\,, \tag{4.3.4}$$

For ultrasound-assisted pseudoelasticity, as $\dot{\sigma} > 0$ and $T = const$, the following formulae are proposed

$$U = U_1\left(\vec{\boldsymbol{S}}_m \cdot \vec{\boldsymbol{N}}\right), \tag{4.3.5}$$

$$r_U = r + U_2|S_m|. \tag{4.3.6}$$

The plots presented constructed via Eqs. (3.1), (3.5)-(3.8) and (4.3.1)-(4.3.6) – demonstrate a good fit of the model to the following experimental data:

(i) Ultrasonic vibrations impulsively added to austenitic transformation result in negative strain jumps. In other words, acoustic energy can initiate strain variations of SMA (Fig. 4.10). The magnitude of the strain jumps increases with the ultrasonic vibration amplitude.

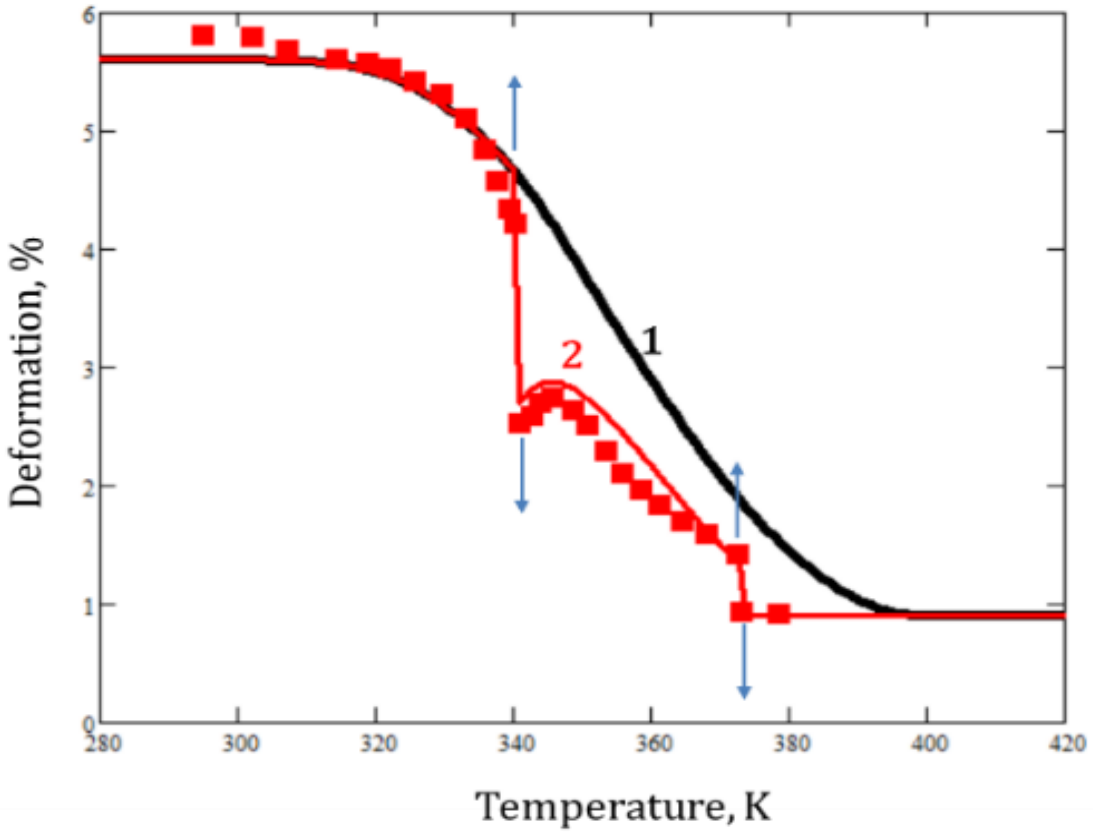

Fig. 4.10 State diagram of NiTi alloy in Deformation-Temperature coordinate. The sample is subjected to uniaxial tension $\sigma = 30$ MPa. The arrows show the moments of switching-on (↑) and switching-off (↓)of ultrasonic vibrations with amplitude 8.3 MPa; ■ –experiment (Rubanik et al., 2008), lines – model.

(ii) The effect of insonation strongly depends on the moment the ultrasound is applied. Acoustic energy has no effect if it acts outside the austenite transformation temperature range. Further, the magnitude of the ultrasound-induced strain jumps is not distributed uniformly within the austenite transformation temperature range. This phenomenon reaches its maximum if the alternate stresses are applied approximately in the middle of the temperature range of phase transformations (Figs. 4.10 and 4.11).

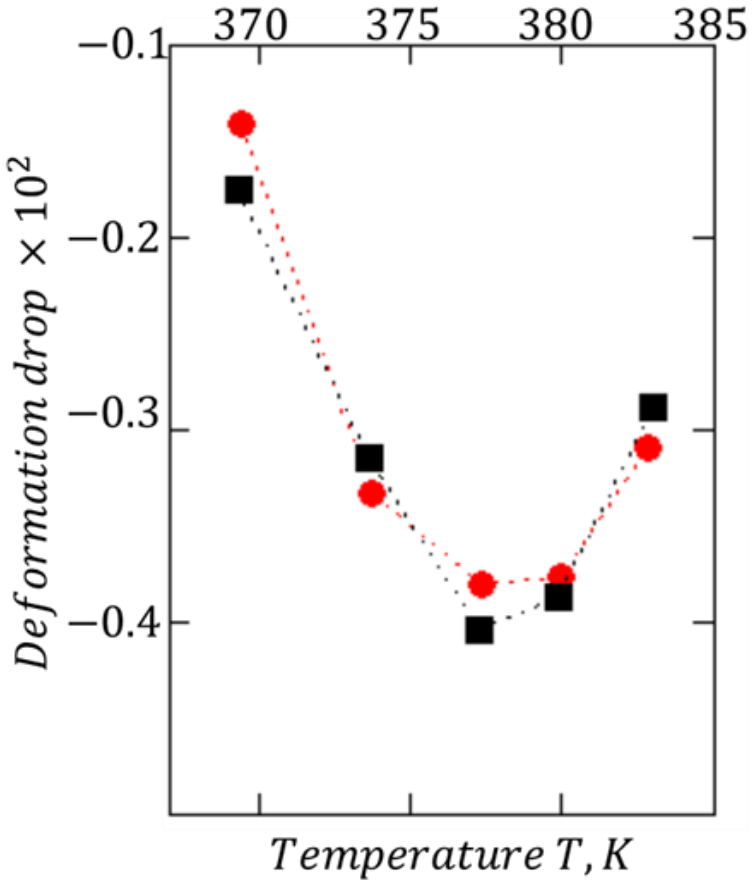

Fig. 4.11 Ultrasound-induced deformation drops in the course of austenitic reverse thermoelastic phase transformation; the amplitude of ultrasonic deformation at every impulse $\varepsilon_m = 5 \times 10^{-5}$ ● – experiment (Steckmann et al. 1999), ■ – model results

(iii) The finish temperature is less than during conventional heating. In other words, the temperature needed to finish the transformation is partially compensated by ultrasound heating. (Fig. 4.10)

(iv) After switching of ultrasound, the further realization of SME occurs according to the reverse transformation kinetics. However, immediately after the ultrasound is off, some "backsliding" in austenitic deformation, a slight increase of deformation, is observed (Fig. 4.10). This aftereffect is assumed to be due to a) the decrease in temperature after ultrasound is off and b) the action of ultrasound which "left a trail" in the form of ultrasound-assisted defect conglomeration, reducing the development of the phase transformations. Therefore, while the central portion of acoustic energy converts irreversibly into the phase deformation increment, some fraction of it recovers.

(v) In the presence of ultrasound, the start stress needed to induce and produce martensite transformation in a pseudoelastic experiment is less than that in the ordinary load (Fig. 4.12).

(vi) At the end of the martensite transformation, the $\sigma \sim \varepsilon$ curve shows steeper kinetics than without ultrasound (Fig. 4.12)

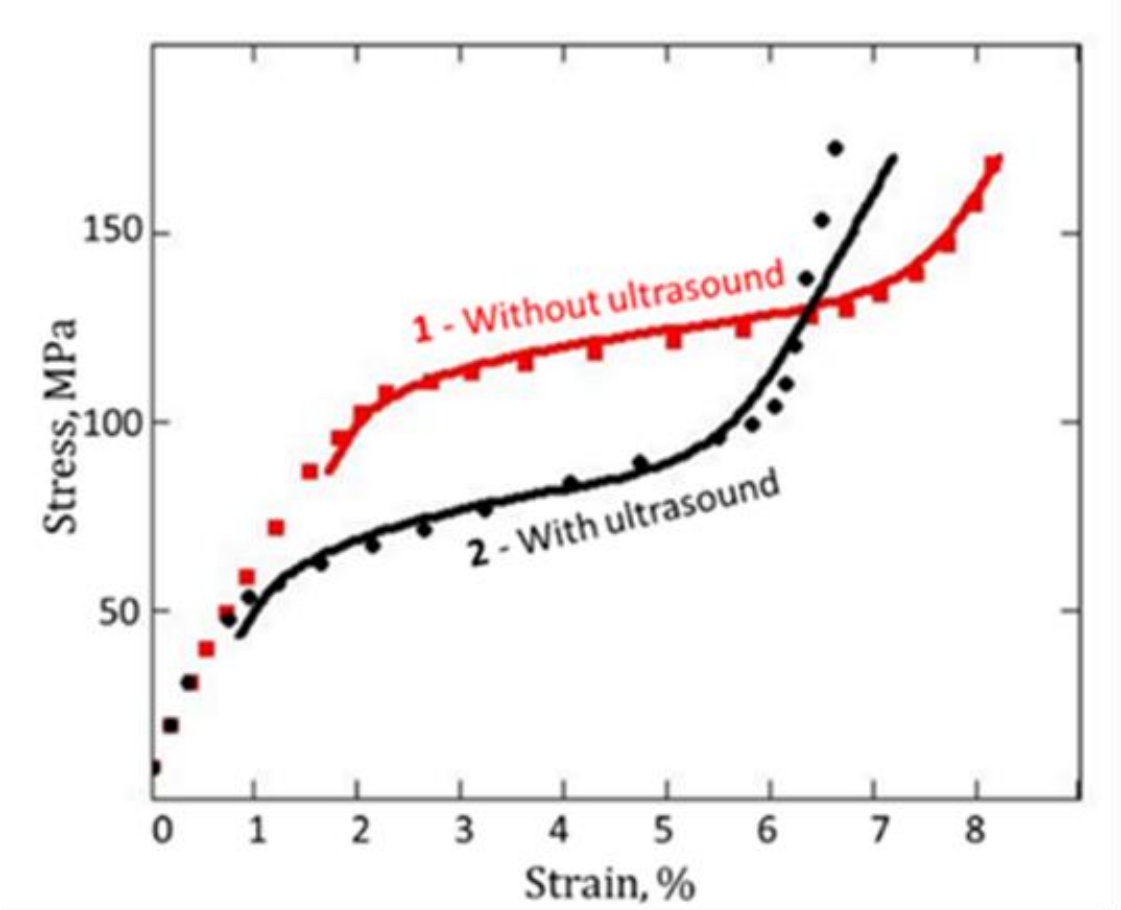

Fig. 4.12 Pseudoelastic σ~ε diagram of NiTiRe alloy at constant temperature ($T_0 = 283$ K) in uniaxial tension: 1 – static loading, 2 – simultaneous action of static and ultrasonic loading ($\sigma_m = 16$ MPa). Lines – model, symbols – experiment (Steckmann et al., 1999).

V. Conclusion

All the objectives set before the dissertation's author are fully implemented. A wide range of issues has been studied and modeled, namely ultrasound-assisted

a) plastic deformation,
b) primary and secondary creep; relaxation processes,
c) phase transformation.

The Synthetic theory, which is taken for a mathematical apparatus, has proved itself as a reliable analytical mechanism to model various non-classical problems in the field of solid mechanics.

List of Publications

[1] Alhilfi, a., & Rusinko, a., (2022), Modelling of ultrasonic temporary and residual effects, *Journal of theoretical and applied mechanics, Sofia*, (52), 64-74. WoS, SCOPUS, Q3**, IF: 0.2**

[2] Alhilfi, A. H., & Rusinko, A. (2022). Ultrasonic temporary softening and residual hardening. *Engineering Review*: 42(2), 101-113. WoS, SCOPUS, Q4

[3] Ali H. Al Hilfi, Andrew Rusinko, (2022), Ultrasonic Temporary Softening And Residual Softening In Terms Of The Synthetic Theory, *AGTECO* 2021, Kecskemét, Hungary, Nov. 25-27, 202. Published in *Gradus* l9(2).

[4] Rusinko, A., & Alhilfi, A. H., (2020), Evolution of loading surface in the ultrasonic field, *Proceedings of the Engineering Symposium at Bánki*, pp. 35-40.

[5] Rusinko, A., & Alhilfi, A. H. (2021). Ultrasound-assisted creep deformation of metals. *Acta Periodica Technologica*, (52), 265-273. WoS, SCOPUS, Q3

[6] Rusinko, A., Alhilfi, A. H., & Rusinko, M. (2022). An analytic description of the creep deformation of metals in the ultrasonic field. *Mechanics of Time-Dependent Materials*, 26(3), 649-661. WoS, SCOPUS, Q2, **IF: 2.538**

[7] Ruszinko, E., & ALHILF, A. (2021). The Effect of Ultrasound on Strain-hardened Metals. *Acta Polytechnica Hungarica*, 18(8), 221-233. SCOPUS, Q2, **IF: 1.71**

[8] Alhilfi, A. H., & Rusinko, A. (2022). Austenite Transformation of Shape Memory Alloys in the Ultrasonic Field. *Mechanics of Solids*, 57(5), 1097-1103. WoS, SCOPUS, Q3, **IF: 0.5**

[9] Alhilfi, A. H., & Rusinko, A. (2022). Effect of Ultrasound on the Pseudoelasticity of Shape Memory Alloys. *Journal of Materials Science and Chemical Engineering*, 10(6), 1-12.

[10] Alhilfi, A. H., & Ruszinkó, E. (2023). Effect of Ultrasound on the Austenite Transformation of Shape Memory Alloys. *Acta Polytechnica Hungarica*, 20(4), 85-101. SCOPUS, Q2, **IF: 1.71**